

Influence of Red Blood Cells on Channel Characterization in Cylindrical Vasculature

Kathan S. Joshi, Dhaval K. Patel, *Member, IEEE*, Shivam Thakker, Miguel López-Benítez, *Senior Member, IEEE*, and Janne J. Lehtomäki, *Member, IEEE*

Abstract—Molecular communication via diffusion (MCvD) expects Brownian motions of the information molecules to transmit information. However, the signal propagation largely depends on the geometric characteristics of the assumed flow model, i.e., the characteristics of the environment, design, and position of the transmitter and receiver, respectively. These characteristics are assumed to be lucid in many ways by either consideration of one-dimensional diffusion, unbounded environment, or constant drift. In reality, diffusion often occurs in blood-vessel-like channels. To this aim, we try to study the effect of the biological environment on channel performance. The Red-Blood Cells (RBCs) found in blood vessels enforces a higher concentration of molecules towards the vessel walls, leading to better reception. Therefore, in this paper we derive an analytical expression of Channel Impulse Response (CIR) for a dispersion-advection-based regime, contemplating the influence of RBCs in the model and considering a point source transmitter and a realistic design of the receiver.

Index Terms—Endothelium Cells, Flow-Based Molecular Communication Systems, Molecule Reception Modelling, Monte-Carlo Simulation, Red-Blood Cells, Targeted Drug Delivery.

I. INTRODUCTION

Contemporary research activities focus on the pro-activeness of disease detection and targeted drug delivery, and Molecular Communication (MC) ought to be one of the leading technologies of the future contributing to the same in a very novel way. It is a promising field because of its nano-networking and biological compatibility. For specific applications, the transmission of information via Electro-Magnetic (EM) waves like those in conventional communication may not be suitable because of the size of the transmitter and receivers are in the order of nanometers or the channel environment may not permit proper utilization of EM waves [1] [2]. This has led to the introduction of a novel paradigm of nanonetworks communication at the molecular level. It is envisioned to have many major revolutionary applications in the field of medical science, such as targeted drug delivery, and early-stage disease detection through continuous monitoring of biomarkers. It could also be used for various industrial applications such as tracking chemical reactors and emissions of pollutants [2] [3]. Nonetheless, accurate and reliable models are required to design the MC system effectively.

Many different channel models are proposed in the current literature, based on the propagation approach used to initiate a communicative connection between the transmitter and receiver as discussed in [2]. In general, for any MC system, the information is transmitted through molecules that are propagated through a fluidic environment and are received by a receiver at the end of the communication process. The MC system is differentiated by the various transmitter-receiver designs, i.e., based on their structural characteristics such as point, surface, volume, and channel environments. The channel environments are diversified based on the type of propagation method that the molecules experience such as free diffusion, molecular motor-driven propagation, propagation through gap junctions, and bacterial motors [1] [4]. Also, different encoding-decoding schemes are deployed based on the quantity, identity, and time of release imparted on molecules to

encode information bits [2]. Nevertheless, Molecular communication via diffusion (MCvD) is considered to be the most visionary aspect of MC because of its biological compatibility, since no specific infrastructure or external energy is required to accomplish communication unlike gap junctions and motor-based propagation. Hence, the scope of this paper is limited to the diffusive model.

A. Previous Related Work

The channel modeling of any MC system excessively depends on the transmitting, propagation, and receiving mechanisms. In the literature, various MC systems have been analyzed considering different transmitter-receiver designs and channel characteristics. An extensive survey based on these parameters is compiled and recorded in [5]. The authors of [6] have studied a rectangular fluidic channel with different flow profiles. In [7], MC systems without flow in a rectangular 2-D environment with reflective walls are considered, with one absorbing wall acting as a receiver. In [8], authors have analyzed a 3-D diffusion molecular system in an unbounded environment without flow over a transparent spherical receiver. The hitting probability of molecules over an absorbing wall is estimated in a 3-D cuboid container without flow in [9]. In [10], authors have considered a propagation model in a vessel-like environment, similar to this work. However, they have not incorporated the advection effect on the molecules existing because of the flow in the environment. In [11], authors have studied a more realistic 3-D propagation model with a feasible receiver design in a duct flow, i.e. similar to blood vessels, with Poiseuille flow, commonly observed in blood vessels. However, they have assumed a uniform distribution of information molecules over the cross-section of the duct flow, which is not reasonable to assume since the concentration of molecules becomes constant over the cross-section after a certain time, as observed in [12] with a similar environment; although the authors in [12], have not reviewed a realistic or feasible design for the receiver.

B. Motivation

The key motivation for this work is to analyze the realistic scenario of an MC system deployed in a blood vessel-like environment. As discussed above, to date, many MC systems have been proposed in a microfluidic duct or cylindrical bounded channel. However, to the best of our knowledge, it does not focus on a feasible and realistic model whether it be the channel characteristic or the receiver design. Hence, in this work we analyze a realistic channel by considering a cylindrical duct filled with fluid exhibiting Poiseuille flow, as reviewed in [5] and references therein, along with a feasible receiver design by assuming it to be similar in structure with endothelial cells present in the endothelium layer of the human blood vessel. Furthermore, we also consider the existence of Red Blood Cells (RBCs) in the channel environment.

The primary principle behind taking such a specific receiver design is that many bodily bio-marker proteins like IL2, IL4, IL6, IL10, and TNF α are received by the endothelial cells present in the endothelium layer. Thus, modeling the reception of these bio-markers is essential since it may aid in the early detection of diseases, as discussed in [13], [14]. Nonetheless, reception at endothelial cells

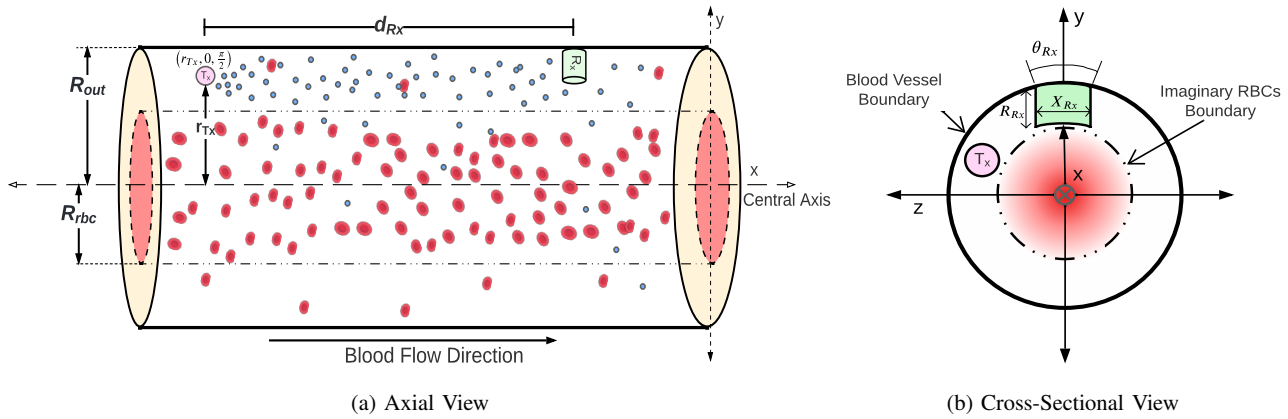


Fig. 1: Network model geometry: (a) axial view, and (b) cross-sectional view. In (a) the outer cylinder represents the blood vessel; the inner cylinder is formed by RBCs radial distribution. In (b) the red gradient shows the radial distribution of RBCs in a cross-sectional view.

is also important to model because of their application in targeted drug delivery. As discussed in [15], endothelial cells are a potent site for pharmacological interventions such as sepsis, Acute Respiratory Distress Syndrome (ARDS), blood clotting disorders, hypertension, diabetes, and tumor growth. Targeted drug delivery to endothelial cells is envisioned to reduce the above-mentioned severe pathological diseases. Hence, it is important to model the molecule reception at endothelial cells. Also, the receiver design has a drastic impact on the channel impulse response. Consequently, generalized receiver designs typically examined in previous literature may not be suitable for targeted drug delivery or early detection of diseases. Thus, it is essential to study an MC system by considering a receiver design in correlation to the structure of endothelial cells. Moreover, monitoring the drug delivery at the targeted site is also important, for which various monitoring methodologies can be employed. For instance, [16] has proposed an ultrasound imaging-based monitoring methodology that can be used to monitor drug distributions in real time. Biosensors can also be used to detect the concentration of drug molecules at the targeted sites. Nevertheless, engineering ultrasound-responsive drug carriers and biosensors can be a challenging task. While these monitoring techniques present interesting research opportunities, this work focuses on deriving the analytical expressions to model the molecule reception at the targeted site.

Additionally, we also contemplate the existence of RBCs in the environment as discussed in [17]. The existence of RBCs or any other molecules larger than the information molecules causes mean-square displacement of the information molecules towards the outer wall of the cylindrical vessel, i.e., a blood vessel in our case. Therefore, it may lead to a false negative channel impulse response when such a system is deployed, if the existence of such larger molecules is not considered in the system.

C. Contribution

In particular, the main contributions of the paper are as follows:

- 1) We propose a novel analytical propagation model for an MC system with diffusion and advection in a bounded human blood vessel-like environment with the interference of third-party molecules into the system. The advection effect is incorporated for Poiseuille flow.
- 2) We formulate an expression to estimate the radial distribution and axial distribution of the information molecules or protein, depending on the context used, considering the elastic collision with the vessel boundary between the transmitter, receiver, and the layer formed by the RBCs.
- 3) We derive an expression for the Channel Impulse Response (CIR) or the fraction of molecules observed by the receiver,

designed similar to endothelial cells present in the endothelial layer in human blood vessels capable of molecule reception on its surface with the considered channel characteristics.

The remainder of this work is organized as follows. In Section II, we introduce the network model and present a preliminary mathematical formulation. Section III includes the mathematical derivation for obtaining the closed-form expression of CIR. In Section IV, we include simulation and numerical results and in Section V we draw the main conclusions resulting from this work and suggest some ideas for future works.

II. SYSTEM MODEL

The considered network model is described in Fig. 1. As shown, we consider a straight impermeable cylindrical model similar to a subsection of blood vessels of radius R_{out} . For the sake of formulating the mathematical analysis more lucidly, we have incorporated a cylindrical coordinate system (r, x, θ) , where $r = \sqrt{y^2 + z^2} \in (0, R_{out}]$ is the radial distance, $x \in (-\infty, \infty)$ is the axial distance, and $\theta \in [0, 2\pi)$ is the azimuth angle. We consider a point transmitter (T_X) at $(r_{Tx}, 0, \pi/2)$ instantaneously releasing N_{Tx} number of molecules at time $t = 0$. Nonetheless, the released particles are transported by a Newtonian fluidic flow attributing properties of a Poiseuille flow and performing Brownian motion in a dispersion-advection-based regime, i.e., the integration of total displacement of molecules combining the effect of cross-sectional and axial diffusion along with non-uniform advection because of flow profile, which is non-uniform over the radial position in the considered propagation model given by:

$$v(r) = v \left(1 - \frac{r^2}{R_{out}^2} \right) \quad (1)$$

where v is the average velocity at the central axis ($r = 0$) and r is any arbitrary radial distance from the center axis of the cylinder. The artificial receiver (R_X) has a shape similar to an endothelial cell in a human blood vessel, i.e., attached to the blood vessel wall, which is the endothelium layer. The receiver is assumed to be capable of detecting the information molecule within its confined volume. The receiver is assumed to be of the cylindrical shape of dimensions R_{Rx} and X_{Rx} , corresponding to height and diameter respectively; the receiver also spans an angle of θ_{Rx} , as shown in Fig. 1. Nevertheless, we assume that the existence of the receiver does not affect the movements of the information molecules. Also, the axial and radial distributions of the information molecules are considered to be not changing across the R_{Rx} , X_{Rx} and θ_{Rx} of the receiver respectively, which is reasonable to assume since the dimensions of the receiver are very small in relation to the vessel radius.

Additionally, we consider an extra imaginary layer of the cylindrical boundary formed due to the existence of RBCs or any larger molecules, which potentially exist in any general MC systems designed in a blood vessel as discussed in [18]. Moreover, it has been shown and verified that the existence of Poiseuille flow in the system leads to the formation of an annulus structure by the particle (RBCs) as seen in [19]. Therefore, the RBCs would form an annulus shape in 3-D, which in general can be assumed to be a hollow cylinder, whose inner radius is defined by R_{rbc} . The thickness of the RBC core region changes across the central axis of the blood vessel as described in [18], however, to this point we have only assumed constant thickness throughout the considered portion of the blood vessel.

To this end, we do consider the standard approximations about information molecules not interacting with each other, and their effect on the velocity of the flow is ignored, due to other negligible physical forces such as the force incurred because of the pressure gradient across the particle due to varying velocity profile, since the dimensions of the molecules are very small [20]. The receiver is assumed to be capable to sense the number of information molecules within its vicinity without discarding the molecules from the environment and drive its decision based on it. Furthermore, since diffusion also exists within the environment along with advection, the motion of each particle could be modeled by the given expressions:

$$\begin{aligned}\Delta X &= v(r)\Delta T + N(0, 2D\Delta T) \\ \Delta Y &= N(0, 2D\Delta T) \\ \Delta Z &= N(0, 2D\Delta T)\end{aligned}\quad (2)$$

Where D is the diffusion coefficient. From Eq. (2), we can easily infer that the radial displacement of molecules is pure because of the diffusion. Hence, the radial displacement is independent of the axial displacement for any molecules. However, the axial displacement is dependent on the radial displacement because of the non-uniform velocity flow profile across the radial space.

III. ANALYSIS OF THE CHANNEL IMPULSE RESPONSE

The channel impulse response for the cylindrical receiver can be obtained as:

$$\begin{aligned}CIR &= n_{hit}(t|r_{Tx}, R_{out}, d_{Rx}) \\ &= \frac{\partial}{\partial t} \int \int \int_{V_{Rx}} p(x, r, t|r_{Tx}, R_{out}) dV_{Rx}\end{aligned}\quad (3)$$

However, in order to estimate the CIR of the considered network model, the joint probability distribution of radial, axial, and time coordinates $p(x, r, t|r_{Tx}, R_{out})$ is to be estimated at first. From Eq. (2) we can infer and express $p(x, r, t|r_{Tx}, R_{out})$ as follow:

$$\begin{aligned}p(x, r, t|r_{Tx}, R_{out}) &= p(r, t|r_{Tx}, R_{out}) \cdot \\ & p(x, t|r_{Tx}, R_{out}, r)\end{aligned}\quad (4)$$

Once we have estimated the CIR, we can easily compute the total number of observed molecules until time t as $N_{hit}(t|r_{Tx}, R_{out}, d_{Rx})$ by integrating $n_{hit}(t|r_{Tx}, R_{out}, d_{Rx})$ over time as:

$$N_{hit}(t|r_{Tx}, R_{out}, d_{Rx}) = \int_0^t n_{hit}(\tau|r_{Tx}, R_{out}, d_{Rx}) d\tau \quad (5)$$

However, we need to find the radial distribution $p(r, t|r_{Tx}, R_{out})$ first, to compute the CIR.

A. Solving for the Radial Distribution $p(r, t|r_{Tx}, R_{out})$

The radial distribution can be formulated by solving Fick's law of diffusion for the probability density function along the radial direction, as shown in [12] and references therein, with appropriate boundary

conditions. Therefore, equation solving for the probability density function can be written as:

$$D\Delta^2 P(r, t|r_{Tx}, R_{out}) = \frac{\partial P(r, t|r_{Tx}, R_{out})}{\partial t} \quad (6)$$

Here, $P(r, t|r_{Tx}, R_{out})$ is the probability density function of molecules. Since the outer boundary or the blood vessel's boundary is considered to be reflecting, the probability of molecules moving normally to the boundary would be equal to zero. Also, as all the molecules are considered to be point release from the transmitter at $t = 0$, the corresponding boundary conditions for Eq. (6) are as follows:

$$\begin{aligned}\left. \frac{\partial P(r, t|r_{Tx}, R_{out})}{\partial r} \right|_{r=R_{out}} &= 0 \\ P(r, t|r_{Tx}, R_{out}) \Big|_{t=0} &= \frac{\delta(r - r_{Tx})}{2\pi r}\end{aligned}\quad (7)$$

Here, $\delta(\cdot)$ is the Dirac delta function. We can solve for $P(r, t|r_{Tx}, R_{out})$ using separation of variables into two new functions $\psi(\theta, r)$, and $\omega(t)$ as follows:

$$P(r, t|r_{Tx}, R_{out}) = \psi(\theta, r)\omega(t) \quad (8)$$

Since our network models follow angular symmetry, $\psi(\theta, r)$ only depends on the radial distance of the molecules from the central axis, i.e., it is independent of the angle θ . Therefore, $\psi(\theta, r)$ can be rewritten as $\psi(r)$. With this, Eq. (6) can be further solved as:

$$D \frac{\Delta \psi(r)}{\psi(r)} = \frac{\omega'(t)}{\omega(t)} \triangleq -\mu^2 \quad (9)$$

Hence, we can derive that:

$$\omega(t) = K e^{-\mu^2 t} \quad (10)$$

Here, K is a constant. Now, $\psi(r)$ can be found by solving the Neumann-eigenvalue problem for the Laplacian operator:

$$\Delta \psi(r) = -\frac{\mu^2}{D} \psi(r) \quad (11)$$

Here, $\frac{\mu^2}{D}$ represents the eigenvalues for the equation. Therefore, we can rewrite the eigenvalue equation for polar coordinates as follows:

$$r^2 \psi(r)'' + r \psi(r)' + \frac{\mu^2}{D} r^2 \psi(r) = 0 \quad (12)$$

The above equation is the second-order Bessel differential equation which has the general solution:

$$\psi(r) = J_0\left(\frac{\mu}{\sqrt{D}}r\right) + cY_0\left(\frac{\mu}{\sqrt{D}}r\right) \quad (13)$$

here, J_n and Y_n are the n th-order Bessel functions of the first and second kind respectively, and c is a constant defined by the boundary condition. The coefficient constant for J_0 is substituted as the overall coefficient K from Eq. (10) as per the boundary conditions described in Eq. (7). Nevertheless, for $t > 0$ the probability density function $P(r, t|r_{Tx}, R_{out})$ converges for $r = 0$, i.e., $(y, z) = (0, 0)$ thus implying $c = 0$. Hence, the second term for Y_0 is zero. Therefore, the general solution for $P(r, t|r_{Tx}, R_{out})$ can be written as:

$$P(r, t|r_{Tx}, R_{out}) = \sum_{n=0}^{\infty} C_n J_0\left(\frac{\mu_n}{\sqrt{D}}r\right) e^{-\mu_n^2 t} \quad (14)$$

Here, C_n and μ_n are defined by the boundary conditions. Therefore, evaluating the first boundary condition as:

$$\left. \frac{\partial P(r, t|r_{Tx}, R_{out})}{\partial r} \right|_{r=R_{out}} = 0 \Rightarrow J_1\left(\frac{\mu_n}{\sqrt{D}}R_{out}\right) = 0 \quad (15)$$

However, the first order Bessel function $J_1(x)$ has an infinite number of roots (β_n). Therefore, $\frac{\mu_n}{\sqrt{D}} R_{out}$ can be expressed as β_n . Using the second boundary condition given in Eq. (7), we can obtain C_n as:

$$C_n = \frac{J_0\left(\beta_n \frac{r_{Tx}}{R_{out}}\right)}{\pi R_{out}^2 J_0^2(\beta_n)} \quad (16)$$

Therefore, the final expression for the probability density function can be written as:

$$P(r, t|r_{Tx}, R_{out}) = \sum_{n=0}^{\infty} \frac{J_0\left(\beta_n \frac{r_{Tx}}{R_{out}}\right)}{\pi R_{out}^2 J_0^2(\beta_n)} J_0\left(\frac{\beta_n}{R_{out}} r\right) e^{-\beta_n^2 \frac{Dt}{R_{out}^2}} \quad (17)$$

Here, β_n is the n^{th} root of the Bessel function of order one, and the first term represents the condition for uniform radial distribution over the cross-section of the vasculature when $t \rightarrow \infty$. However, practically it takes much less time for the molecules to reach uniform radial distribution. Therefore, the final probability distribution can be expressed as follows:

$$p(r, t|r_{Tx}, R_{out}) = 2\pi r \cdot P(r, t|r_{Tx}, R_{out}) \quad (18)$$

So far in the presented analysis, we have not considered the existence of third-party molecules in the system. However, while considering third-party molecules, (i.e., RBCs in our assumption in the system) we simply cannot consider Eq. (18) as the final radial distribution. A non-negligible change can be observed because of this additional assumption. In particular, the RBCs in our context form an annulus (ring-shaped), and mostly all the molecules in consideration would exist outside of this formed annulus structure depending on the absorption and reflection rate of the additional layer formed by the RBCs, i.e., the boundary of the annulus structure. Hence, the actual total number of information molecules existing within the annulus structure P_{inside} can be written as:

$$P_{inside} = \rho \int_0^{R_{rbc}} \sum_{n=0}^{\infty} C_n J_0\left(\frac{\beta_n}{R_{out}} r\right) e^{-\beta_n^2 \frac{Dt}{R_{out}^2}} dr \quad (19)$$

where R_{rbc} is the radius of the annulus structure, and ρ is the correlation coefficient which varies with the absorption and reflection rate as follows:

$$\rho \propto \text{absorption rate}, \quad \rho \propto \frac{1}{\text{reflection rate}} \quad (20)$$

As discussed ρ is contingent on the absorption rate and reflection rate which can be explained as follows. When molecules collide with the RBC layer it gets either reflected back inside the layer, i.e., the molecule itself has collided with an RBC molecule and it is reflected back (since the density of RBC is higher than the molecules), or it gets absorbed, which means that while diffusing towards the RBC layer molecule escaped the layer and did not collide with any RBC molecule in the process. Likewise, a similar scenario can be observed when the molecule collides with the RBC layer from outside. In reality, the absorption and reflection rate itself depends on the number of RBCs present in the blood, which can be termed as the concentration or percentage volume of RBCs in the blood, i.e., hematocrit. Hence, the value of ρ varies with the hematocrit value. Nevertheless, the value of ρ also depends on the size of the information molecule relative to the size of the RBCs ($8\mu\text{m}$). However, due to mathematical simplicity, we are not considering the size as a factor in the analysis. Rather a general case of information molecules smaller than the RBCs is considered.

Therefore, the effective radial probability density can be separated for two different scenarios, i.e., for $r > R_{rbc}$ and $r < R_{rbc}$, which

can be expressed as:

$$P(r, t|r_{Tx}, R_{out}) = \begin{cases} P_{mean}(r) + P_{outside}, & \text{if } r \geq R_{rbc} \\ \rho \cdot P_{mean}(r), & \text{if } r < R_{rbc} \end{cases} \quad (21)$$

where $P_{mean}(r)$ can be defined by Eq. (17) and $P_{outside}$ is defined as the probability density of molecules outside of the annulus structure formed by the RBCs, which can be formulated as below:

$$P_{outside} = \int_0^{R_{rbc}} \sum_{n=0}^{\infty} C_n J_0\left(\frac{\beta_n}{R_{out}} r\right) e^{-\beta_n^2 \frac{Dt}{R_{out}^2}} dr - \rho \int_0^{R_{rbc}} \sum_{n=0}^{\infty} C_n J_0\left(\frac{\beta_n}{R_{out}} r\right) e^{-\beta_n^2 \frac{Dt}{R_{out}^2}} dr \quad (22)$$

In particular, the probability density of molecules for $r < R_{rbc}$ is defined by multiplying it with ρ is based on the law of mass conservation. Since no explicit assumption is taken for the degradation of molecules and no new molecules are transmitted after time $t = 0$, thus, the number of molecules pushed outside of the RBC boundary is rejigged by the decrease in the number of molecules remaining inside of the RBC boundary because of its reflective nature. Now, before solving for $P_{outside}$, it is important to note that the integration property of the Bessel function (equation 6.511.6 of [21]) is given as:

$$\int_0^a J_0(x) dx = a J_0(a) + \frac{\pi a}{2} [J_1(a) H_0(a) - J_0(a) H_1(a)] \quad (23)$$

where $H(\cdot)$ is a Struve function (such functions are solutions to inhomogeneous Bessel differential equations). Hence, we could utilize Eq. (23) in order to solve Eq. (22) by substituting the input to the Bessel function as $U = \frac{\beta_n}{R_{out}} r$. By applying the above variable change we can rewrite Eq. (22) by limit and derivative change as follows:

$$P_{outside} = \int_0^{\frac{\beta_n R_{rbc}}{R_{out}}} \sum_{n=0}^{\infty} C_n \frac{R_{out}}{\beta_n} J_0(U) e^{-\beta_n^2 \frac{Dt}{R_{out}^2}} dU - \rho \int_0^{\frac{\beta_n R_{rbc}}{R_{out}}} \sum_{n=0}^{\infty} C_n \frac{R_{out}}{\beta_n} J_0(U) e^{-\beta_n^2 \frac{Dt}{R_{out}^2}} dU \quad (24)$$

$$= (1 - \rho) \sum_{n=0}^{\infty} A_n \left[R_{rbc} J_0\left(\frac{\beta_n}{R_{out}} R_{rbc}\right) + \frac{\pi R_{rbc}}{2} \left[J_1\left(\frac{\beta_n}{R_{out}} R_{rbc}\right) H_0\left(\frac{\beta_n}{R_{out}} R_{rbc}\right) - J_0\left(\frac{\beta_n}{R_{out}} R_{rbc}\right) H_1\left(\frac{\beta_n}{R_{out}} R_{rbc}\right) \right] \right] \quad (25)$$

Here, $A_n = C_n e^{-\beta_n^2 \frac{Dt}{R_{out}^2}}$. Henceforth, we can combine Eq. (21) and Eq. (25) to compute the net effective $P(r, t|r_{Tx}, R_{out})$. Therefore, the net radial distribution $p(r, t|r_{Tx}, R_{out})$ can be easily obtained as:

$$p(r, t|r_{Tx}, R_{out}) = \begin{cases} 2\pi r [P_{mean}] + P_{outside}, & \text{if } r \geq R_{rbc} \\ 2\pi r [\rho \cdot P_{mean}], & \text{if } r < R_{rbc} \end{cases} \quad (26)$$

It is worth noting that for a shorter duration of time, the molecules may or may not even reach the RBC layer. In such a case, there is no need to bifurcate the radial distribution into two different scenarios, i.e., Eq. (26) can directly be used to evaluate the radial distribution for the case $r < R_{rbc}$ without scaling it with ρ . Since the effect of the existence of RBCs only matters if the molecules at least collide with them. However, it is essential to approximate the time ω after which a sufficient number of molecules have collided with the RBC layer several times and the influence of RBCs in the system becomes vital to consider because of a better understanding of molecular physics and its

substantial application in the healthcare. Now, physical interpretation of ω could be made as the time after which a subsequent number of molecules must have passed the RBCs boundary. Therefore, ω can be approximated as below:

$$\int_0^{R_{rbc}} 2\pi r \cdot P(r, \omega | r_{Tx}, R_{out}) dr < \int_{R_{rbc}}^{R_{out}} 2\pi r \cdot P(r, \omega | r_{Tx}, R_{out}) dr \quad (27)$$

B. Solving for the Axial Distribution $p(x, t | r, r_{Tx}, R_{out})$

As the axial distribution of the molecules is dependent on the radial distribution $p(r, t | r_{Tx}, R_{out})$, it is essential to have prior knowledge of the radial distribution. Furthermore as demonstrated in [11] [12], one can assume the molecules to be uniformly distributed across the cross-section after a certain time \hat{t} . As discussed in [22], if the radial distribution of the molecules is uniform then the axial distribution $p(x, t | r, r_{Tx}, R_{out})$ can be written as:

$$p(x, t | r, r_{Tx}, R_{out}) = \frac{1}{\sqrt{4\pi D_{eff} t}} e^{-\left(\frac{x - \frac{vt}{2}}{2\sqrt{D_{eff} t}}\right)^2} \quad (28)$$

which is equivalent to a one-dimensional Brownian motion with an effective diffusion coefficient D_{eff} . As discussed in [23], Taylor-Aris effective diffusion coefficient D_{eff} followed by [22] can be written as:

$$D_{eff} = D \left(1 + \frac{1}{48} \left(\frac{v R_{out}}{2D} \right)^2 \right) \quad (29)$$

As explained before, to achieve uniform radial distribution, the channel should have either a high diffusion coefficient, leading to faster dispersion of molecules in the radial space or the duct could have a small radius. However, a small amount of time \hat{t} is required before $p(r, t | r_{Tx}, R_{out})$ becomes uniform. Furthermore, since \hat{t} is very small as compared to the total time of diffusion, one can assume uniform distribution in the radial space. Henceforth, $p(x, t | r, r_{Tx}, R_{out})$ can be expressed by Eq. (28) for uniform radial distribution. Nevertheless, before achieving uniform distribution, the displacement of individual molecules is different because of the irregular radial displacement ($t < \hat{t}$). Hence, we need to estimate the mean displacement of a molecule and substitute it into Eq. (28). The mean displacement of a molecule $x_{mean}(t)$ for time t can be calculated as follows:

$$x_{mean}(t) = \int_0^t \int_0^{R_{out}} p(r, t | r_{Tx}, R_{out}) v(r) dr d\tau \quad (30)$$

After evaluating $x_{mean}(t)$ the axial distribution followed by Eq. (28) could be rewritten as follow:

$$p(x, t | r, r_{Tx}, R_{out}) = \frac{1}{\sqrt{4\pi D_{eff} t}} e^{-\left(\frac{x - x_{mean}(t)}{2\sqrt{D_{eff} t}}\right)^2} \quad (31)$$

C. Solving for the Fraction of molecules within the receiver $N_{hit}(t | r_{Tx}, R_{out}, d_{Rx})$

We have estimated the values of both radial and axial components, which can be further used to calculate the channel impulse response for the cylindrical receiver using Eq. (3). Thus, the $n_{hit}(t | r_{Tx}, R_{out}, d_{Rx})$ (CIR) could be estimated by differentiating the following expression with respect to time, as mentioned above.

$$N_{hit}(t | r_{Tx}, R_{out}, d_{Rx}) = \iint_{V_{Rx}} p(x, r, t | r_{Tx}, R_{out}) dV_{Rx} \quad (32)$$

Note that it is irrelevant to consider the distribution of molecules in radial space for $r < R_{rbc}$ if $R_{rbc} \leq R - R_{Rx}$. Therefore, we only consider the spatial distribution for $r \geq R_{rbc}$. Therefore, the final

expression for $N_{hit}(t | r_{Tx}, R_{out}, d_{Rx})$ can be written as follows:

$$N_{hit}(t | r_{Tx}, R_{out}, d_{Rx}) = -\frac{\theta_{Rx} R_{Rx} (R_{Rx} - 2R_{out})}{4\pi R_{out}^2} \left\{ \text{Erf} \left[\frac{\frac{X_{Rx}}{2} + d_{Rx} - \sum_{n=0}^{\infty} Z_n}{2\sqrt{D_e t}} \right] + \text{Erf} \left[\frac{\frac{X_{Rx}}{2} - d_{Rx} + \sum_{n=0}^{\infty} Z_n}{2\sqrt{D_e t}} \right] \right\} \quad (33)$$

where Z_n is:

$$Z_n = R_{out} v \left(1 - e^{-\frac{D t \beta_n^2}{R_{out}^2}} \right) J_0 \left(\frac{r_{Tx} \beta_n}{R_{out}} \right) \left\{ R_{rbc} (\rho - 1) \beta_n^2 \left(J_0 \left(\frac{R_{rbc} \beta_n}{R_{out}} \right) \left(\pi H_1 \left(\frac{R_{rbc} \beta_n}{R_{out}} \right) - 2 \right) - \pi J_1 \left(\frac{R_{rbc} \beta_n}{R_{out}} \right) H_0 \left(\frac{R_{rbc} \beta_n}{R_{out}} \right) \right) + 12\pi R_{out} J_2(\beta_n) \right\} \quad (34)$$

IV. SIMULATION AND NUMERICAL RESULTS

In this section, we describe our simulation framework which was developed to verify our analytical expressions derived in Section III. We conducted 3-D Monte Carlo simulations to verify the radial distribution and number of received molecules rate. The simulation followed Brownian motion where the position of each molecule is updated at each time step according to Eq. (2). Furthermore, accurate positions of each molecule are recorded throughout the simulation. All the simulation parameters are listed in Table I. To validate our

TABLE I: System Parameters used for Numerical and Simulation Results

Symbols	Value	Description
Δt	$10^{-3} s$	Simulation time step
N_{tx}	10^5	Number of released molecules
D	$10^{-10} m/s^2$	Diffusion coefficient
v	$10^{-2} m/s$	Blood flow velocity
R_{out}	$15 \times 10^{-6} m$	Blood Vessel Radius
R_{rbc}	$5 \times 10^{-6} m$	Inner radius formed by RBC
d_{Rx}	$5 \times 10^{-3} m$	Axial distance between T_x and R_x
r_{Tx}	$0 \mu m$	Radial displacement of the T_x

analytical results, we have plotted the distribution of molecules on the Y-axis and the radial displacement on the X-axis. Different plots are generated for discrete time instances, namely $t = 200ms$ and $t = 2s$. The results can be seen in Figs. 2, 3, 4, and 5.

In general, we can observe the discontinuity in Figs. 2, 3, 4, and 5 depending upon the varied values of ρ and different time instances considered. This is plausible as well, since the radial distribution current normal to the imaginary boundary formed by the RBCs, would abruptly change about the boundary in practice. Also, we have plotted the radial distribution in two different scenarios, uniform ($t = 2s$) and non-uniform ($t = 200ms$), across the cross-sectional area of the cylindrical vessel.

In Fig. 2 and Fig. 3, the radial distribution is plotted for different values of ρ and t . Specifically, for $\rho = 0.3$, $t = 200ms$, and for $\rho = 0.7$, $t = 2s$, respectively. As shown, the proposed analytical equations are verified by Monte Carlo simulations. Also, as can be seen in Figs. 2 and 3, the value of ρ greatly affects the discontinuous nature of the radial distribution. Due to the fact that as the value of ρ increases, the absorption rate and reflection rate of molecules getting absorbed into the imaginary RBCs boundary and getting reflected back, respectively;

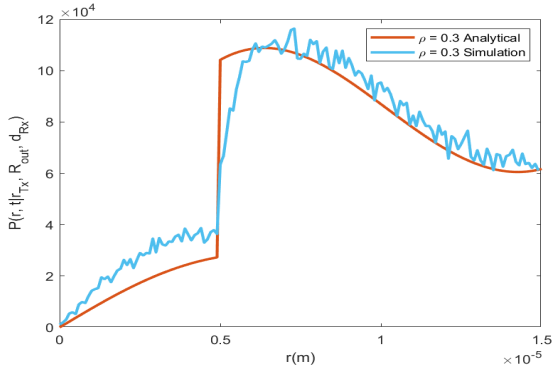


Fig. 2: Radial distribution $p(r, t | r_{Tx}, R_{out})$ at $\rho = 0.3$ at non-uniform distribution ($t = 200ms$).

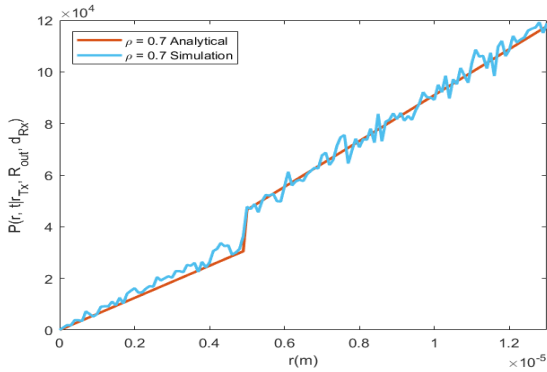


Fig. 3: Radial distribution $p(r, t | r_{Tx}, R_{out})$ $\rho = 0.7$ at uniform distribution ($t = 2s$).

start becoming akin to each other, and eventually leading to $\rho = 1$ in which the absorption rate is equal to the reflection rate. Henceforth, the greater difference between the absorption rate and reflection rate leads to a smaller value of ρ ; which results in a higher probability of molecules being pushed outside of the RBCs boundary than being collided back inside. Furthermore, this discontinuity remains constant even after the uniform radial distribution is achieved $t = 200ms$. To this point, we can conclude a drastic increase and decrease in the distribution of the molecules for $r \geq R_{rbc}$ and $r < R_{rbc}$, respectively. It is also worth noting that as the value of $\rho \rightarrow 0$, the discontinuity about R_{rbc} as well as the distribution of the molecules outside of the annulus structure increases gradually. Nevertheless, we can deduce that it is not ideal or realistic to consider the channel environment completely free of third-party molecules, if so it would lead to significant false negative errors in the radial distribution.

In Figs. 4 and 5, the radial distribution is represented to depict the backward compatibility of our proposed analytical formula with the existing literature. Note that $\rho = 1$ is a special case. In this case, even if the RBCs or any other third-party larger molecules exist within the system, their effect would be nullified as the absorption and reflection rates would be equal. Nevertheless, in this case, the system would be exactly identical to the system described in literature [12], except for the different receiver design. Hence, for this case ($\rho = 1$) we get the exact same results as discussed in [12], which shows the backward compatibility of our newly derived analysis with the existing literature. Furthermore, backward compatibility is observed in both scenarios, uniform and non-uniform distribution. It was also observed that the existence of the third-party molecules does not affect the time taken for the radial distribution to attain uniformity in the radial space.

In Fig. 6, the fraction of molecules within the receiver is plotted for $\rho = 0.7$. As the receiver is assumed to be capable of detecting the number of molecules inside its proximity, the fraction

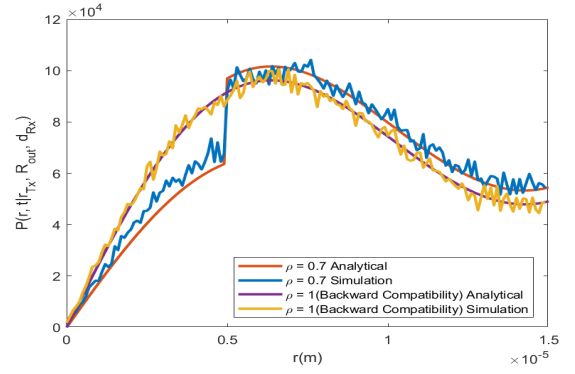


Fig. 4: Radial distribution $p(r, t | r_{Tx}, R_{out})$ at $\rho = 0.7$ and $\rho = 1$ for non-uniform distribution ($t = 200ms$).

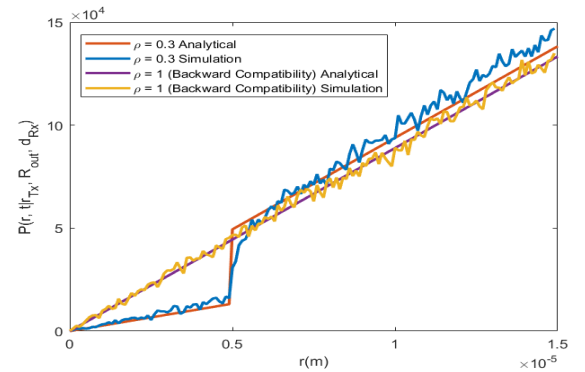


Fig. 5: Radial distribution $p(r, t | r_{Tx}, R_{out})$ at $\rho = 0.3$ and $\rho = 1$ for non-uniform distribution ($t = 2s$).

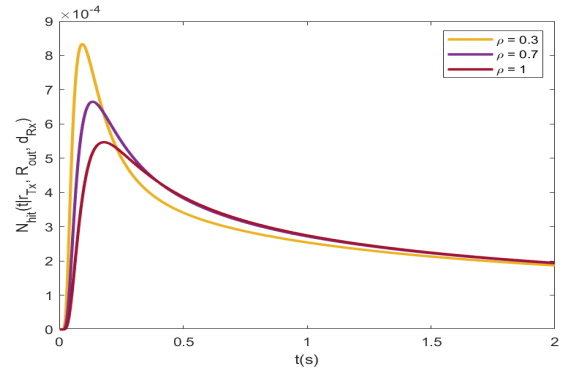


Fig. 6: Fraction of molecules within the receiver $N_{hit}(t | r_{Tx}, R_{out}, d_{Rx})$ at varied ρ .

of molecules $N_{hit}(t | r_{Tx}, R_{out}, d_{Rx})$ can directly be obtained by integrating the spatial PDF of the molecule over the receiver volume. Nevertheless, the receiver's proximity can be characterised by $(X_{Rx}, R_{Rx}, \theta_{Rx})$, the axial, radial, and azimuth dimensions; where $X_{Rx} = R_{out}/2, R_{Rx} = R_{out}/2, \theta_{Rx} = \pi/6$. It was observed that with decreasing values of ρ the reception of molecules at the receiver increases, which is a plausible explanation because as the value of ρ decreases there is a higher probability of molecules being outside the RBC region, i.e., near to the blood vessels boundary. That is because more molecules are pushed outside of the RBC layer than getting reflected back inside. Table II shows the closeness of our analytical results with the simulation for Figs. 2-5 using three metrics, namely, Root Mean Squared Error (RMSE), Median Absolute Percentage Error (MAPE), and Kolmogorov-Smirnov distance (KS_{dist}), respectively. As observed through all the metrics, the analytical and simulation curves are quite close to each other. The relatively high MAPE value in

TABLE II: Closeness Metrics of Analytical Results with the Simulation

Figure	Curve Parameters	RMSE	MAPE	KS_{dist}
Fig. 2	$\rho = 0.3, t = 200ms$	10.57×10^3	9.054%	3.336%
Fig. 3	$\rho = 0.7, t = 2s$	2.90×10^3	3.057%	0.660%
Fig. 4	$\rho = 0.7, t = 200ms$	4.64×10^3	4.859%	1.830%
Fig. 4	$\rho = 1, t = 200ms$	2.77×10^3	3.056%	0.727%
Fig. 5	$\rho = 0.3, t = 2s$	5.38×10^3	4.867%	1.223%
Fig. 5	$\rho = 1, t = 2s$	2.60×10^3	2.910%	0.367%

Fig. 2, is due to the transition zone around $r = 0.5 \times 10^{-5}m$. However, the RMSE for this figure is about one order of magnitude lower than the values in the figure itself and, additionally, the KS_{dist} is around 3% as well, which suggests an overall good accuracy over the whole domain of Fig. 2. Furthermore, the distribution current normal to the RBCs boundary is large at high ρ ($=0.3$) in non-uniform distribution ($t = 200ms$). Similarly, the decrease in current at uniform distribution ($t = 2s$) exhibits closeness in analytical and simulation curves (Fig. 5).

V. CONCLUSION AND FUTURE WORK

This work has presented a novel analysis of a channel environment with the existence of a third-party molecule that is relatively larger than the information molecules (i.e., the RBCs in this case). The model provides a more accurate and supports a more realistic scenario as compared to previous research, which does not consider such anomalous existence of other particles in the environment with a realistic design of the receiver. Nonetheless, the proposed analysis is generic, and can also be applied to any other MC system, where the channel fluid follows a Poiseuille flow along with the existence of third-party molecules larger in size than the molecules of interest in a cylindrical vessel.

In this work, we have shown that the existence of larger molecules drastically increases and decreases the radial displacement of molecules across the radial space of the micro-cylindrical channel, greatly affecting the CIR of the MC system with the receiver attached to the inner surface of the channel, i.e similar to endothelium cells in the human body. We observe that the fraction of molecules received by such a receiver increases as $\rho \rightarrow 0$. Hence, the potential existence of such molecules in the system should not be ignored. For instance, in a system design problem for targeted drug delivery, If RBCs are not taken into account, a patient may end up consuming higher dosages of the drug, which may lead to adverse side effects. On the other hand, by taking RBCs' existence in the blood vessel into account (which is also evident in nature) we could deliver a higher fraction of the drug to the targeted sites, with minimal side effects (less dosage of drug). To conclude, the presented analytical results are a good match to the performed 3D Monte Carlo Simulations. Also, the results provide accurate results, with pragmatic assumptions for the fraction of molecules within a realistic designed receiver, i.e., targeted to get the estimation of the effect of medicinal drugs on the infected endothelial cells of human blood vessels.

The future extension of this work could be the incorporation of multiple transmitters and receivers into the system, along with the third-party molecules. Such scenarios are of significant interest to study as they lead to direct application in emerging modern healthcare applications.

REFERENCES

[1] T. Nakano, A. W. Eckford, and T. Haraguchi, *Molecular communication*. Cambridge University Press, 2013.

[2] N. Farsad, H. B. Yilmaz, A. Eckford, C.-B. Chae, and W. Guo, "A comprehensive survey of recent advancements in molecular communication," *IEEE Communications Surveys & Tutorials*, vol. 18, no. 3, pp. 1887–1919, 2016.

[3] L. P. Giné and I. F. Akyildiz, "Molecular communication options for long range nanonetworks," *Computer Networks*, vol. 53, no. 16, pp. 2753–2766, 2009.

[4] M. Gregori and I. F. Akyildiz, "A new nanonetwork architecture using flagellated bacteria and catalytic nanomotors," *IEEE Journal on selected areas in communications*, vol. 28, no. 4, pp. 612–619, 2010.

[5] V. Jamali, A. Ahmadzadeh, W. Wicke, A. Noel, and R. Schober, "Channel modeling for diffusive molecular communication—a tutorial review," *Proceedings of the IEEE*, vol. 107, no. 7, pp. 1256–1301, 2019.

[6] A. O. Bicen and I. F. Akyildiz, "Molecular transport in microfluidic channels for flow-induced molecular communication," in *2013 IEEE International Conference on Communications Workshops (ICC)*. IEEE, 2013, pp. 766–770.

[7] M. R. Bhatnagar *et al.*, "Molecular channel characterization for a rectangular container with reflecting and absorbing boundaries," *IEEE Communications Letters*, vol. 24, no. 2, pp. 234–238, 2019.

[8] M. Saeed, M. Maleki, P. Mohseni, and H. R. Bahrami, "An analytical propagation model for diffusion-based molecular communication systems," *IEEE Transactions on Molecular, Biological and Multi-Scale Communications*, 2021.

[9] M. R. Bhatnagar *et al.*, "Diffusion channel characterization for a cuboid container: Some insights into the role of dimensionality and fluid boundaries," in *2020 International Conference on Signal Processing and Communications (SPCOM)*. IEEE, 2020, pp. 1–5.

[10] M. Turan, M. Ş. Kuran, H. B. Yilmaz, I. Demirkol, and T. Tugcu, "Channel model of molecular communication via diffusion in a vessel-like environment considering a partially covering receiver," in *2018 IEEE International Black Sea Conference on Communications and Networking (BlackSeaCom)*. IEEE, 2018, pp. 1–5.

[11] W. Wicke, T. Schwering, A. Ahmadzadeh, V. Jamali, A. Noel, and R. Schober, "Modeling duct flow for molecular communication," in *2018 IEEE Global Communications Conference (GLOBECOM)*. IEEE, 2018, pp. 206–212.

[12] F. Dinc, B. C. Akdeniz, A. E. Pusane, and T. Tugcu, "A general analytical approximation to impulse response of 3-d microfluidic channels in molecular communication," *IEEE transactions on nanobioscience*, vol. 18, no. 3, pp. 396–403, 2019.

[13] L. Felicetti, M. Femminella, and G. Reali, "A molecular communications system for the detection of inflammatory levels related to covid-19 disease," *IEEE Transactions on Molecular, Biological and Multi-Scale Communications*, vol. 7, no. 3, pp. 165–174, 2021.

[14] S. Thakker, D. K. Patel, K. S. Joshi, and M. Lopez-Benitez, "Modelling the impact of multiple pro-inflammatory cytokines using molecular communication," in *2022 National Conference on Communications (NCC)*. IEEE, 2022, pp. 291–296.

[15] P. M. Glassman, J. W. Myerson, L. T. Ferguson, R. Y. Kiseleva, V. V. Shuvaev, J. S. Brenner, and V. R. Muzykantor, "Targeting drug delivery in the vascular system: Focus on endothelium," *Advanced drug delivery reviews*, vol. 157, pp. 96–117, 2020.

[16] F. Conversano, E. Casciaro, R. Franchini, A. Lay-Ekuakille, and S. Casciaro, "A quantitative and automatic echographic method for real-time localization of endovascular devices," *IEEE Transactions on Ultrasonics, Ferroelectrics, and Frequency Control*, vol. 58, no. 10, pp. 2107–2117, 2011.

[17] J. Tan, A. Thomas, and Y. Liu, "Influence of red blood cells on nanoparticle targeted delivery in microcirculation," *Soft matter*, vol. 8, no. 6, pp. 1934–1946, 2012.

[18] D. A. Fedosov, B. Caswell, A. S. Popel, and G. E. Karniadakis, "Blood flow and cell-free layer in microvessels," *Microcirculation*, vol. 17, no. 8, pp. 615–628, 2010.

[19] O. Aouane, M. Sega, B. Bäuerlein, K. Avila, and J. Harting, "Inertial focusing of a dilute suspension in pipe flow," *Physics of Fluids*, vol. 34, no. 11, p. 113312, 2022.

[20] H. Bruus, *Theoretical microfluidics*. Oxford university press, 2007, vol. 18.

[21] I. S. Gradshteyn and I. M. Ryzhik, *Table of integrals, series, and products*. Academic press, 2014.

[22] R. F. Probstein, *Physicochemical hydrodynamics: an introduction*. John Wiley & Sons, 2005.

[23] R. Aris, "On the dispersion of a solute in a fluid flowing through a tube," *Proceedings of the Royal Society of London. Series A. Mathematical and Physical Sciences*, vol. 235, no. 1200, pp. 67–77, 1956.